Bulletin of Electrical Engineering and Informatics
Vol. 15, No. 3, June 2026, pp. 2045~2053
ISSN: 2302-9285, DOI: 10.11591/eei.v15i3.11081

Modified integral sliding mode speed controller for predictive stator flux and torque controlled induction motor drive

Hau Huu Vo[1], Dat Vinh Phat Tran[2]
[1]Modeling Evolutionary Algorithms Simulation and Artificial Intelligence, Faculty of Electrical and Electronics Engineering, Ton Duc Thang University, Ho Chi Minh City, Vietnam
[2]Faculty of Electrical and Electronics Engineering, Ton Duc Thang University, Ho Chi Minh City, Vietnam

Article Info

Article history:

Received Jul 23, 2025
Revised Mar 17, 2026
Accepted Apr 1, 2026

Keywords:

Induction motor drive
Integral sliding mode
Motor model
Predictive control
Speed controller

ABSTRACT

The paper deals with utilization of integral sliding mode (SM) in speed controller of predictive torque and flux control (PTC) of induction motor (IM). At first, the model-based prediction of the motor torque and stator flux is presented. Then, the voltage vector of the inverter is selected to minimize the errors of the torque and the flux. The proportional-integral (PI) speed controller is used to provide the reference torque for the torque controller. However, the PI speed controller is not achieved high performance especially in cases of high load torque and low speed commands. Then, the integral SM one is employed to enhance the speed control performance. Simulations of two speed controllers in PTC drive are carried out. Evaluations using criterions relevant to speed error confirm the expected performance of the integral SM speed controller.

Corresponding Author:

Hau Huu Vo
Modeling Evolutionary Algorithms Simulation and Artificial Intelligence
Faculty of Electrical and Electronics Engineering, Ton Duc Thang University
No. 19 Nguyen Huu Tho Street, Tan Hung Ward, Ho Chi Minh City, Vietnam
Email: vohuuhau@tdtu.edu.vn

1. INTRODUCTION

Induction motors (IMs) play an important role in industrial fields [1]. In order to achieve high-performance, field-oriented control, direct torque control, and model predictive control (MPC) were presented [2]-[6]. In order to enhance the MPC performance, various techniques were developed [7]-[10]. Cost functions were utilized to regulate the flux and torque, and decrease the harmonic [7]. An observer integrated the MPC increased the stability at low speed [8]. The voltage vectors-based cost function were employed to improve the drive [9]. A power-based MPC removed flux angle computation [10].

Versions of sliding mode (SM) theory were selected to control complex systems [11]-[19]. The hover system was controlled by the SM control in case of disturbances [11]. In switched reluctance drive, the fractional SM using nonsingular surface was employed under parameter uncertainties and disturbances [12]. To improve performance in frequency control of a power system, an integral was deployed [13]. Parameters of the SM controllers were optimized by the metaheuristic algorithm in the control of highly nonlinear system [14]. To stabilize the load frequency, an observer was integrated to estimate variables for the non-reaching-phase SMC [15]. The space vector pulse width modulation (PWM) directly-driven synchronous motor control was improved by the prescribed SM [16]. An exoskeleton was robustly controlled by a non-singular SM [17]. The SMC was utilized in maximum torque per ampere control for synchronous motor [18]. In order to obtain robustness and desired response, a nonlinear switching function was added to minimize the

integral time absolute error (ITAE) performance index [19]. For the disturbed IM controls, the SM algorithms were widely utilized [20]–[25].

The super-twisting SM estimation enhanced the performance IM drive [20]. A nonlinear term added to model predictive torque and flux control (MPTC) using sliding, reduced the uncertainties effect [21]. An ultra-local model based on an integral SM observer eliminated the uncertainties [22]. The discrete SM increased the sensorless IM drive accuracy at high-speed region [23]. The flux linkage was modified by the SM in the linear IM MPC [24]. An adaptive SM reduced the chattering at flux weakening region and the settling time [25]. Next, the state-space model of the IM is presented. The model is utilized to predict both the stator flux and the motor torque for the MPTC [26]. Unlike [21], [22] SMs were used to predict the models for increasing the robustness to uncertainty, the SM control is employed in speed controller. Boundary of the disturbance is estimated. Finally, the integral SM control is deployed to address the uncertainties because it enhances the conventional SMC technique by removing the reaching phase, increasing the robustness, guaranteeing disturbance-free during initialization. The structure of the paper includes sections: section 1 introduction, section 2 proposed SM predictive torque and flux control, section 3 simulation and discussion, and section 4 conclusion.

2. PROPOSED SLIDING MODE PREDICTIVE TORQUE AND FLUX CONTROL

Proposed MPTC drive integrated integral SM speed controller is shown in Figure 1. The state-space representation of the IM is given by (1):

$$\dot{X} = AX + BU_s \tag{1}$$

where, X is state of the system containing components of the stator current and rotor flux vectors; U_s is input of the system consisting of components of the stator voltage vector; A and B are system matrix and input matrix:

$$X = \begin{bmatrix} i_{s\alpha} \\ i_{s\beta} \\ \psi_{r\alpha} \\ \psi_{r\beta} \end{bmatrix}^T ; U_s = \begin{bmatrix} u_{s\alpha} \\ u_{s\beta} \end{bmatrix}; A = \begin{bmatrix} a_1 & 0 & a_2 & a_3 n_p \omega_m \\ 0 & a_1 & -a_3 n_p \omega_m & a_2 \\ \frac{L_m R_r}{L_r} & 0 & -\frac{R_r}{L_r} & -n_p \omega_m \\ 0 & \frac{L_m R_r}{L_r} & n_p \omega_m & -\frac{R_r}{L_r} \end{bmatrix}; B = \begin{bmatrix} \frac{1}{\sigma L_s} & 0 \\ 0 & \frac{1}{\sigma L_s} \\ 0 & 0 \\ 0 & 0 \end{bmatrix} \tag{2}$$

where, ω_m is motor speed; n_p is number of pole pairs; L_m, L_r, and L_s are magnetizing, rotor and stator inductances; R_r and R_s are rotor and stator resistances; remaining parameters of A and B are calculated according to (3):

$$\sigma = 1 - \frac{(L_m^2)}{(L_s L_r)}; a_1 = -\frac{(L_m^2 R_r + L_r^2 R_s)}{(\sigma L_s L_r^2)}; a_2 = \frac{L_m R_r}{(\sigma L_s L_r^2)}; a_3 = \frac{L_m}{(\sigma L_s L_r)} \tag{3}$$

Motor torque T_e and simplified motor dynamics are computed (4):

$$T_e = \left(\frac{(3 n_p L_m)}{(2 L_r)}\right)(i_{s\beta}\psi_{r\alpha} - i_{s\alpha}\psi_{r\beta}); J_m\left(\frac{d\omega_m}{dt}\right) = T_e - T_L - B_m\omega_m \tag{4}$$

where, T_L is load torque; J_m is motor inertia; and B_m is rotational damping constant of the motor.

In order to obtain the state at the h^{th} instant, the rotor flux vector components are estimated by the estimation and prediction using IM model (EPUM) block as (5) and (6):

$$\psi_{s\alpha}^h = \psi_{s\alpha}^{h-1} + t_p(u_{s\alpha}^h - R_s i_{s\alpha}^h); \psi_{s\beta}^h = \psi_{s\beta}^{h-1} + t_p(u_{s\beta}^h - R_s i_{s\beta}^h) \tag{5}$$

$$\psi_{r\alpha}^h = \left(\frac{L_r}{L_m}\right)\psi_{s\alpha}^h - \left(\frac{i_{s\alpha}^h}{a_3}\right); \psi_{r\beta}^h = \left(\frac{L_r}{L_m}\right)\psi_{s\beta}^h - \left(\frac{i_{s\beta}^h}{a_3}\right) \tag{6}$$

where, t_p is predictive period of the PTC drive. For more accurate predicting, the Heun's method is utilized [6]:

$$X_{p,v}^{h+1} = t_p\left(AX^h + BU_{s,v}^{h+1}\right) + X^h; X_v^{h+1} = 0.5 t_p A\left(X_{p,v}^{h+1} - X^h\right) + X_{p,v}^{h+1} \tag{7}$$

where, v=1 to 7 are one of seven voltage vectors for utilized 2-level inverter. To obtain the inputs of the minimization of cost function (MOCF), the motor torque and the stator flux magnitude are computed:

$$\psi_{s\alpha,v}^{h+1} = \left(\frac{L_m}{L_r}\right)\psi_{r\alpha,v}^{h+1} + \left(\frac{L_m}{(a_3 L_r)}\right) i_{s\alpha,v}^{h+1}; \psi_{s\beta,v}^{h+1} = \left(\frac{L_m}{L_r}\right)\psi_{r\beta,v}^{h+1} + \left(\frac{L_m}{(a_3 L_r)}\right) i_{s\beta,v}^{h+1} \quad (8)$$

$$\psi_{s,v}^{h+1} = \sqrt{\left(\psi_{s\alpha,v}^{h+1}\right)^2 + \left(\psi_{s\beta,v}^{h+1}\right)^2}; T_{e,v}^{h+1} = 1.5 n_p (i_{s\beta,v}^{h+1}\psi_{s\alpha,v}^{h+1} - i_{s\alpha,v}^{h+1}\psi_{s\beta,v}^{h+1}) \quad (9)$$

Two computed quantities are employed to obtain cost function Z_v:

$$Z_v = \left|T_e^{ref} - T_{e,v}^{h+1}\right| + \left(\frac{k_\psi T_n}{\psi_{s,n}}\right)\left|\psi_s^{ref} - \psi_{s,v}^{h+1}\right| \quad (10)$$

where: k_ψ is positive weighting factor that is trial and error; T_n and ψ_{sn} are rated torque and rated stator flux magnitude, respectively. The MOCF block outputs the voltage vector v that minimizes the cost function [26].

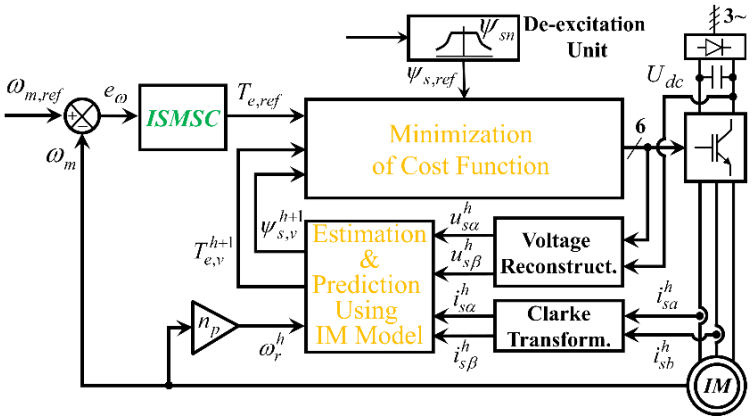

Figure 1. The MPTC drive integrated integral SM speed controller

For the SM control, commonly-used switching function S and its time derivative are:

$$S = \dot{e}_\omega + k e_\omega; \dot{S} = \ddot{\omega}_{m,ref} - \ddot{\omega}_m + k\dot{\omega}_{m,ref} - k\dot{\omega}_m \quad (11)$$

where, e_ω=($\omega_{m,ref}$–ω_m) is speed error, k>0. By replacing (4) into (11), the derivative is simplified as (12):

$$\dot{S} = F - u \quad (12)$$

where, F and u are respectively the disturbance term and control law of the system (4):

$$F = \ddot{\omega}_{m,ref} - \ddot{\omega}_m + k\dot{\omega}_{m,ref} + \left(\frac{kB_m}{J_m}\right)\omega_m + \left(\frac{k}{J_m}\right)T_L; u = \left(\frac{k}{J_m}\right)T_e \quad (13)$$

The disturbance is assumed to be bounded: $|F| \le F_M$. In order to asymptote the error e_ω to zero, Lyapunov function L and its time derivative must satisfy:

$$L = \frac{S^2}{2}; \dot{L} = S\dot{S} \le -k_c|S| \quad (14)$$

where: k_c>0. The control law is chosen as (15):

$$u = g \times sign(S) \quad (15)$$

where: g>0. By substituting (12) and (15) into the left side of (14), following inequality is obtained:

$$\dot{L} \le |S|F_M - S \times g \times sign(S) \quad (16)$$

Equating the right side of (14) and (16), leads to:

$$g = F_M + k_c, for S \neq 0 \tag{17}$$

In the SM S=0, equivalent control law u_{eq} is derived to satisfy the condition dS/dt=0:

$$\dot{S} = F - u_{eq} = 0 \Rightarrow u_{eq} = F \tag{18}$$

Assuming that $T_{e,ref}$=T_e, the reference motor torque is computed as (19):

$$T_{e,ref} = \begin{cases} \frac{J_m(F_M + k_c)sign(S)}{k}, for\ S \neq 0 \\ \frac{J_m F}{k}, for\ S = 0 \end{cases} \tag{19}$$

For the integral SM, an auxiliary control law is defined to compensate for the disturbance boundary:

$$u = u_1 + u_2; V = S - Z; \dot{Z} = -u_2 \tag{20}$$

The derivative of the function V is given by:

$$\dot{V} = (F - u) - (-u_2) = F - u_1 \tag{21}$$

Similarly, definition of Lyapunov function L_1, condition of its time derivative, and selection of the control law u_1, are presented in (22):

$$L_1 = \frac{V^2}{2}; \dot{L}_1 = V\dot{V} \leq -k_c|V|; u_1 = (F_M + k_c)sign(V), for\ V \neq 0 \tag{22}$$

In the SM V=0, equivalent control u_{1eq} is also found to guarantee the condition $\dot{V} = 0$:

$$\dot{V} = F - u_{1eq} = 0 \Rightarrow u_{1eq} = F; T_{e1,ref} = \begin{cases} \frac{J_m(F_M + k_c)sign(V)}{k}, for\ V \neq 0 \\ \frac{J_m F}{k}, for\ V = 0 \end{cases} \tag{23}$$

To move S to zero, thanks to (12), (20), and (23), the control law u_2 is chosen as (24):

$$\dot{S} = -u_2; u_2 = k_2 S(k_2 > 0) \tag{24}$$

3. SIMULATION AND DISCUSSION

Parameters of the simulated motor are given in Table 1. Simulations of the MPTC drive for two speed controllers: the proportional-integral (PI) and the integral sliding mode (ISMC) ones are implemented at T_L={0.55T_n, 0.95T_n} and $\omega_{m,ref}$={200 rpm, 20 rpm, 2 rpm}. In order to evaluate the performance of speed controllers, undershoot/overshoot (UOS) and normalized integral time absolute speed error are utilized:

$$ITAE_n = (\int_0^3 t|e_\omega(t)|dt)/\omega_{m,ref} \tag{25}$$

Table 1. IM parameters [2]

Symbol	Quantity	Value	Symbol	Quantity	Value
T_n	Rated torque	14.8 N·m	J_m	Moment of inertia	0.0047 kg·m^2
ψ_{sn}	Rated stator flux	0.78 Wb	R_s	Stator resistance	3.179 Ω
$\omega_{m,n}$	Rated speed	1420 rpm	R_r	Rotor resistance	2.118 Ω
P_n	Rated power	2.2 kW	L_s=L_r	Stator and rotor inductances	0.209 H
n_p	Number of pole pairs	2	L_m	Magnetizing inductance	0.192 H

Figures 2-4 show all simulated cases. Two speed controllers provide higher UOSs at larger load torques. The UOS seems negligible in the case of the ISMC (see enlarged image in Figures 2-4). For the PI, the UOS rapidly increases with load torque magnitude. Tables 2-5 list all UOSs for operating modes including starting (0 s-0.5 s), forward motoring (0.5 s-1 s), forward unloading (1 s-1.5 s), reverse (1.5 s-2 s), reverse loading (2 s-2.5 s), and reverse unloading (2.5 s-3 s) ones.

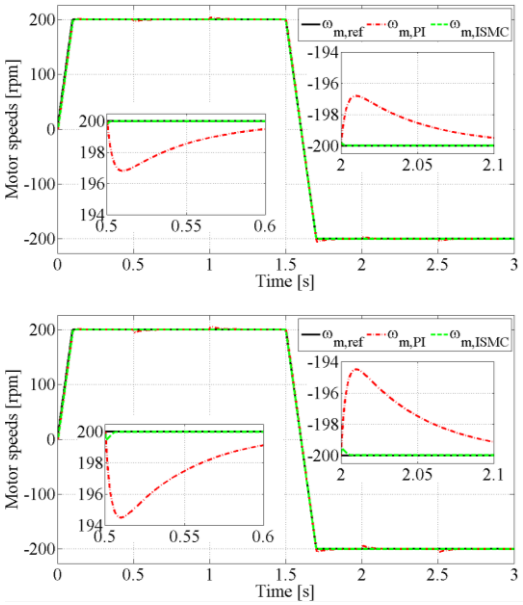

Figure 2. Speed responses at ω_{ref}=200 rpm, T_L=0.55 T_n (upper), and T_L =0.95 T_n (lower)

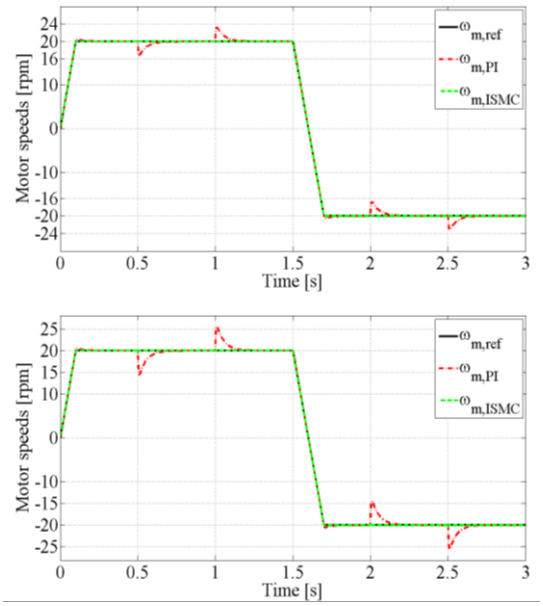

Figure 3. Speed responses at ω_{ref}=20 rpm, T_L=0.55 T_n (upper), and T_L=0.95 T_n (lower)

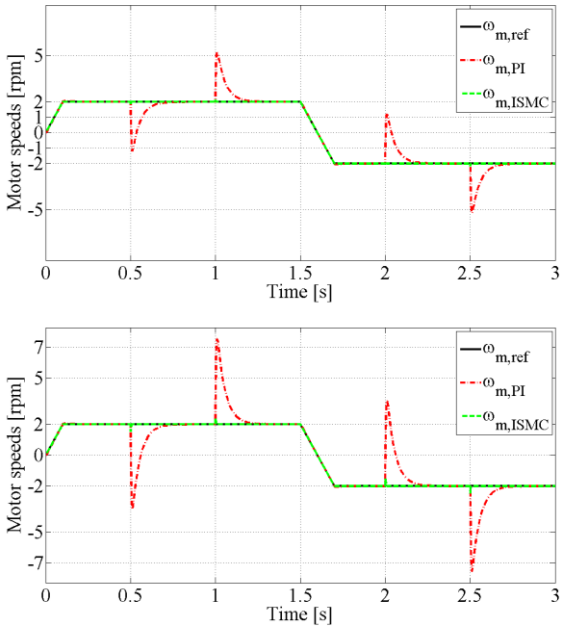

Figure 4. Speed responses at ω_{ref}=2 rpm, T_L=0.55 T_n (upper), and T_L=0.95 T_n (lower)

Table 2. Overshoot [%] at starting mode

Controller	$\omega_{m,ref}$=200	$\omega_{m,ref}$=20	$\omega_{m,ref}$=2
PI	4.68	3.05	2.94

Table 3. Undershoot/overshoot [%] at forward motoring/forward unloading modes

	Forward motoring						Forward unloading					
T_L	$\omega_{m,ref}$=200		$\omega_{m,ref}$=20		$\omega_{m,ref}$=2		$\omega_{m,ref}$=200		$\omega_{m,ref}$=20		$\omega_{m,ref}$=2	
	PI	ISMC	PI	ISMC	PI	ISMC	PI	ISMC	PI	ISMC	PI	ISMC
0.55 T_n	1.6	0.08	16	0.77	160	7.7	1.6	0.06	16	0.76	160	7
0.95 T_n	2.76	0.25	27.6	2.31	276	23	2.76	0.2	27.6	2.26	276	21.8

Table 4. Overshoot [%] at reverse mode

T_L	$\omega_{m,ref}$ =200		$\omega_{m,ref}$ =20		$\omega_{m,ref}$ =2	
	PI	ISMC	PI	ISMC	PI	ISMC
0.55 T_n	2.86	0.21	2.86	0.025	2.86	0.025
0.95 T_n	2.86	0.23	2.86	0.025	2.87	0.026

Table 5. Undershoot/overshoot [%] at reverse loading/reverse unloading modes

T_L	Forward motoring						Forward unloading					
	$\omega_{m,ref}$ =200		$\omega_{m,ref}$ =20		$\omega_{m,ref}$ =2		$\omega_{m,ref}$ =200		$\omega_{m,ref}$ =20		$\omega_{m,ref}$ =2	
	PI	ISMC	PI	PI	ISMC	ISMC	PI	ISMC	PI	PI	ISMC	ISMC
0.55 T_n	1.59	0.09	16	0.73	160	7.5	1.59	0.07	16	0.72	160	7.7
0.95 T_n	2.75	0.23	27.6	2.63	276	23.4	2.76	0.2	27.6	2	276	23.4

In the starting mode (see Table 2), the UOS is approximately the same for both controllers. For the remaining modes (see Tables 3-5), the ISMC yields a 90.8%-99.1% reduction in the UOS. The reason for this improvement is that the motor response of the ISMC is significantly faster than that of the PI (see torque peaks at times 0.5 s, 1 s, 2 s, and 2.5 s in lower sub-images of Figure 5). It can be seen that the switching function and the auxiliary one approach the sliding line very quickly after leaving the surface due to the change of load (see extra figure in Figure 6).

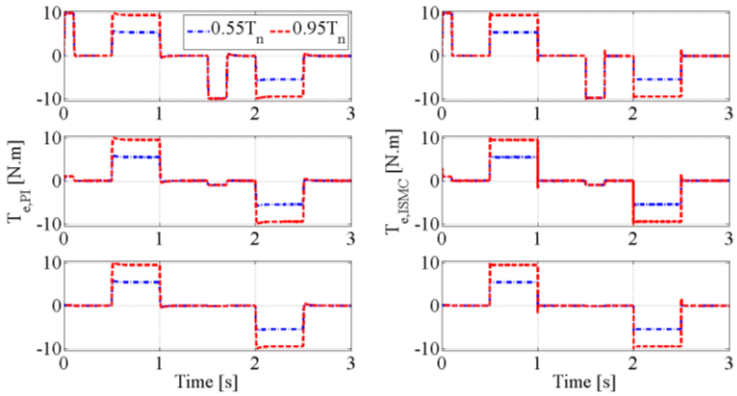

Figure 5. Motor torque responses at ω_{ref}=200 rpm (upper), ω_{ref}=20 rpm (center), and ω_{ref}=2 rpm (lower)

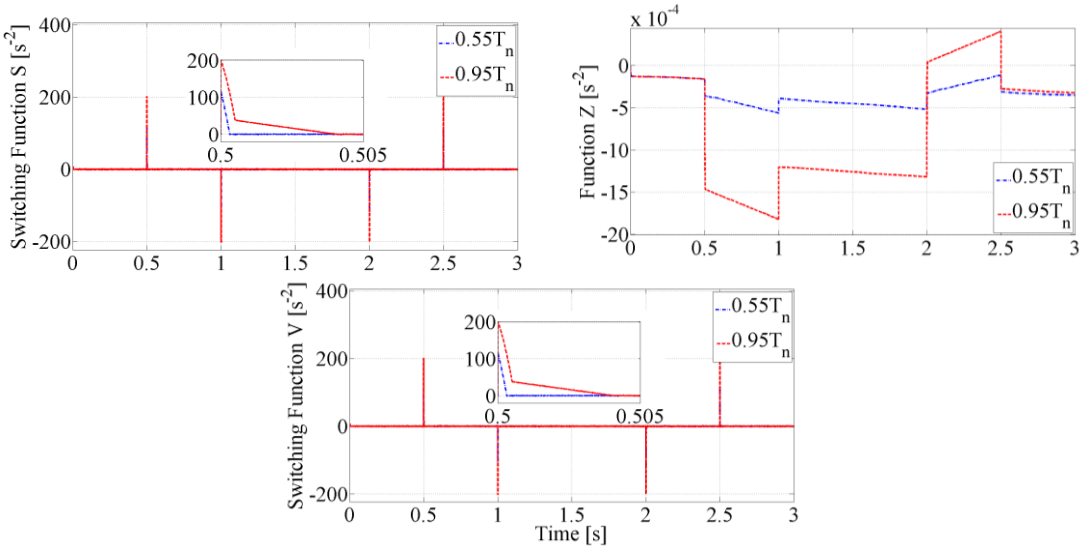

Figure 6. Switching function at ω_{ref}=2 rpm

Unlike conventional SMC [20], ISMC reduces chattering almost completely due to its ability to eliminate the reaching phase. Table 6 indicates that the $ITAE_n$ index for the ISMC is also decreased 96.9%-99.8% compared to that for the PI. Although evaluated indices are reduced significantly, the UOS can be up to 23.4% at lowest speed command and highest load torque (see Table 5).

Table 6. $ITAE_n \times 10^{-3}$ [s^2]

T_L	$\omega_{m,ref}$ =200		$\omega_{m,ref}$ =20		$\omega_{m,ref}$ =2	
	PI	ISMC	PI	ISMC	PI	ISMC
0.55 T_n	12.9	0.41	62	0.11	574	1.00
0.95 T_n	17.1	0.43	104	0.37	987	3.36

4. CONCLUSION

The MPTC utilizing the PI and the integral SM speed controllers were presented and simulated in regions of low speed command and high load torque. The ISMC dedicates the benefits up to 99.1% and 99.8% in the UOS and the $ITAE_n$ indices, respectively. The proposed ISMC almost eliminates the reaching phase but the load torque needs to be estimated. In addition, there is still chattering phenomenon and high UOS at highest load torque and lowest speed command. The twisting or super-twisting or non-singular terminal SM algorithms and the load torque estimators can be employed to address the problems. MPC techniques such as flux control method can be deployed to eliminate weighting factor tuning for the stator flux. Design and analysis based on the robustness to uncertainties of parameters and measured quantities such as stator current and rotor time constant, can be developed. The proposed method can be implemented using embedded controllers and inverter platforms.

ACKNOWLEDGMENTS

Authors acknowledge Ton Duc Thang University, Ho Chi Minh City, Vietnam for supporting this research.

FUNDING INFORMATION

Authors state no funding involved.

AUTHOR CONTRIBUTIONS STATEMENT

This journal uses the Contributor Roles Taxonomy (CRediT) to recognize individual author contributions, reduce authorship disputes, and facilitate collaboration.

Name of Author	C	M	So	Va	Fo	I	R	D	O	E	Vi	Su	P	Fu
Hau Huu Vo	✓	✓	✓	✓	✓	✓	✓	✓	✓	✓	✓	✓	✓	✓
Dat Vinh Phat Tran		✓				✓				✓	✓			

C : **C**onceptualization
M : **M**ethodology
So : **So**ftware
Va : **Va**lidation
Fo : **Fo**rmal analysis
I : **I**nvestigation
R : **R**esources
D : **D**ata Curation
O : Writing - **O**riginal Draft
E : Writing - Review & **E**diting
Vi : **Vi**sualization
Su : **Su**pervision
P : **P**roject administration
Fu : **Fu**nding acquisition

CONFLICT OF INTEREST STATEMENT

Authors state no conflict of interest.

DATA AVAILABILITY

Data availability is not applicable to this paper as no new data were created or analyzed in this study.

REFERENCES

[1] M. G. Simoes, "A Concise History of Induction Motor Drives - Part 1 [History]," *IEEE Electrification Magazine*, vol. 11, no. 2, pp. 5–11, Jun. 2023, doi: 10.1109/MELE.2023.3264888.

[2] H. H. Vo, D. V. P. Tran, T. Q. Thieu, T. A. Le, C. S. T. Dong, and P. Brandstetter, "Sliding Mode PWM-Direct Torque Controlled Induction Motor Drive with Kalman Filtration of Estimated Load," *Journal of Advanced Engineering and Computation*, vol. 5, no. 4, pp. 264–275, Dec. 2021, doi: 10.55579/jaec.202154.342.

[3] K. Rahman *et al.*, "Field-Oriented Control of Five-Phase Induction Motor Fed from Space Vector Modulated Matrix Converter," *IEEE Access*, vol. 10, pp. 17996–18007, 2022, doi: 10.1109/ACCESS.2022.3142014.

[4] V. S. R. Chagam and S. Devabhaktuni, "Enhanced Low-Speed Characteristics With Constant Switching Torque-Controller-Based DTC Technique of Five-Phase Induction Motor Drive With FOPI Control," *IEEE Transactions on Industrial Electronics*, vol. 70, no. 11, pp. 10789–10799, Nov. 2023, doi: 10.1109/TIE.2022.3227275.

[5] S. Mahfoud, N. El Ouanjli, A. Derouich, A. El Idrissi, A. Hilali, and E. Chetouani, "Higher performance enhancement of direct torque control by using artificial neural networks for doubly fed induction motor," *e-Prime - Advances in Electrical Engineering, Electronics and Energy*, vol. 8, Jun. 2024, doi: 10.1016/j.prime.2024.100537.

[6] G. A. Pangratz, W. C. A. Pereira, Y. R. Novaes, J. A. Alves, and M. Rivera, "Model Predictive Control of Cascaded H-Bridge Inverters Driving Induction Motors," in *2023 IEEE 8th Southern Power Electronics Conference and 17th Brazilian Power Electronics Conference (SPEC/COBEP)*, Florianopolis, Brazil: IEEE, Nov. 2023, pp. 1–8, doi: 10.1109/SPEC56436.2023.10408292.

[7] A. Bhowate, M. V. Aware, and S. Sharma, "Predictive Torque Control of Five-Phase Induction Motor Drive Using Successive Cost Functions for CMV Elimination," *IEEE Transactions on Power Electronics*, vol. 36, no. 12, pp. 14133–14141, Dec. 2021, doi: 10.1109/TPEL.2021.3089741.

[8] N. D. Nguyen, N. N. Nam, C. Yoon, and Y. Il Lee, "Speed Sensorless Model Predictive Torque Control of Induction Motors Using a Modified Adaptive Full-Order Observer," *IEEE Transactions on Industrial Electronics*, vol. 69, no. 6, pp. 6162–6172, Jun. 2022, doi: 10.1109/TIE.2021.3094493.

[9] I. Oliani, R. Figueiredo, L. F. N. Lourenco, A. Pelizari, and A. J. S. Filho, "Robust Predictive Current Control Using Discrete-Time Integral Action for Induction Motors," *IEEE Journal of Emerging and Selected Topics in Power Electronics*, vol. 11, no. 6, pp. 5766–5773, Dec. 2023, doi: 10.1109/JESTPE.2023.3316828.

[10] J. Zhang *et al.*, "A Simple and Effective Predictive Power Control for Induction Motor Drives," *IEEE Transactions on Power Electronics*, vol. 39, no. 11, pp. 14898–14908, Nov. 2024, doi: 10.1109/TPEL.2024.3404069.

[11] B. Ouahab, M. A. Alouane, and F. Boudjema, "Robust Sliding Mode Control Design for a 3-DOF Hover System," in *2022 International Conference of Advanced Technology in Electronic and Electrical Engineering (ICATEEE)*, M'sila, Algeria: IEEE, Nov. 2022, pp. 1–6, doi: 10.1109/ICATEEE57445.2022.10093762.

[12] A. A. Hagras, "Adaptive Fractional Order Sliding Mode Speed and Current Control for Switched Reluctance Motor," *Acta Polytechnica Hungarica*, vol. 19, no. 5, pp. 85–106, 2022, doi: 10.12700/APH.19.5.2022.5.5.

[13] D. H. Tuan, J. Pidanic, V. V. Huynh, V. H. Duy, and N. H. K. Nhan, "Sliding Mode Without Reaching Phase Design for Automatic Load Frequency Control of Multi-Time Delays Power System," *IEEE Access*, vol. 12, pp. 110052–110063, 2024, doi: 10.1109/ACCESS.2024.3441092.

[14] C. A. Bojan-Dragos, R. E. Precup, A. I. Szedlak-Stinean, R. C. Roman, E. L. Hedrea, and E. M. Petriu, "Sliding Mode and Super-Twisting Sliding Mode Control Structures for SMA Actuators," in *2023 European Control Conference (ECC)*, Bucharest, Romania: IEEE, Jun. 2023, pp. 1–6, doi: 10.23919/ECC57647.2023.10178281.

[15] C. T. Nguyen, C. T. Hien, and V. D. Phan, "Observer-based single phase robustness load frequency sliding mode controller for multi-area interconnected power systems," *Bulletin of Electrical Engineering and Informatics*, vol. 13, no. 5, pp. 3147–3154, Oct. 2024, doi: 10.11591/eei.v13i5.7893.

[16] J. Zhou and D. Tian, "Prescribed Performance Sliding Mode Controller for SVPWM Directly Driven PMSM," in *2024 IEEE 18th International Conference on Advanced Motion Control (AMC)*, Kyoto, Japan: IEEE, Feb. 2024, pp. 1–6, doi: 10.1109/amc58169.2024.10505708.

[17] M. D. Hassen, I. Laamiri, and N. Bouguila, "A Robust Adaptive Non-Singular Terminal Sliding Mode Control: Application to an Upper-Limb Exoskeleton with Disturbances and Uncertain Dynamics," *Information Technology and Control*, vol. 53, no. 1, pp. 171–186, Mar. 2024, doi: 10.5755/j01.itc.53.1.33752.

[18] X. Zhang *et al.*, "Maximum Torque per Ampere Control for IPMSM Based on Sliding Mode Extremum Seeking Control Without Steady-State Oscillation," *IEEE Journal of Emerging and Selected Topics in Power Electronics*, vol. 14, no. 1, pp. 1203-1214, Feb. 2026, doi: 10.1109/JESTPE.2025.3635915.

[19] M. Pietrala, P. Leśniewski, and A. Bartoszewicz, "An ITAE Optimal Sliding Mode Controller for Systems with Control Signal and Velocity Limitations," *Acta Mechanica et Automatica*, vol. 17, no. 2, pp. 230–238, Jun. 2023, doi: 10.2478/ama-2023-0026.

[20] M. M. Amin, F. F. M. El-Sousy, O. A. Mohammed, G. A. A. Aziz, and K. Gaber, "MRAS-Based Super-Twisting Sliding-Mode Estimator Combined With Block Control and DTC of Six-Phase Induction Motor for Ship Propulsion Application," *IEEE Transactions on Industry Applications*, vol. 57, no. 6, pp. 6646-6658, Nov.-Dec. 2021, doi: 10.1109/TIA.2021.3115088.

[21] V. Kousalya, R. Rai, and B. Singh, "Sliding Model-Based Predictive Torque Control of Induction Motor for Electric Vehicle," *IEEE Transactions on Industry Applications*, vol. 58, no. 1, pp. 742–752, Jan. 2022, doi: 10.1109/TIA.2021.3131973.

[22] M. S. Mousavi, S. A. Davari, V. Nekoukar, C. Garcia, and J. Rodriguez, "Integral Sliding Mode Observer-Based Ultralocal Model for Finite-Set Model Predictive Current Control of Induction Motor," *IEEE Journal of Emerging and Selected Topics in Power Electronics*, vol. 10, no. 3, pp. 2912–2922, Jun. 2022, doi: 10.1109/JESTPE.2021.3110797.

[23] T. Wang, B. Wang, Y. Yu, and D. Xu, "Discrete Sliding-Mode-Based MRAS for Speed-Sensorless Induction Motor Drives in the High-Speed Range," *IEEE Transactions on Power Electronics*, vol. 38, no. 5, pp. 5777-5790, May 2023, doi: 10.1109/TPEL.2023.3236024.

[24] M. F. Elmorshedy, D. J. Almakhles, and F. F. M. El-Sousy, "Modified Primary Flux Linkage for Enhancing the Linear Induction Motor Performance Based on Sliding Mode Control and Model Predictive Flux Control," *IEEE Access*, vol. 11, pp. 26184–26198, 2023, doi: 10.1109/ACCESS.2023.3257231.

[25] B. Cavus and M. Aktas, "A New Adaptive Terminal Sliding Mode Speed Control in Flux Weakening Region for DTC Controlled Induction Motor Drive," *IEEE Transactions on Power Electronics*, vol. 39, no. 1, pp. 449–458, Jan. 2024, doi: 10.1109/TPEL.2023.3326383.

[26] T. M. Krupa, S. Koraddi, and A. B. Raju, "Model Predictive Torque Control of Induction Motor for Electric Vehicle Application," in *2024 International Conference on Innovation and Novelty in Engineering and Technology (INNOVA)*, Vijayapura, India, 2024, pp. 1-5, doi: 10.1109/INNOVA63080.2024.10846978.

BIOGRAPHIES OF AUTHORS

Hau Huu Vo received his Ph.D. degree in field of Electrical Machines, Apparatus and Drives from Faculty of Electrical Engineering and Computer Science, Technical University of Ostrava, Czech Republic in 2017. He is currently a Lecturer at Faculty of Electrical and Electronics Engineering (FEEE), Ton Duc Thang University (TDTU). He is a member of Ho Chi Minh City Automation Association and Ho Chi Minh City Electrical Engineering Association. He has published 15 journal papers. His research interests are high-performance control, sensorless control, intelligent, and robust control of electrical drives. He can be contacted at email: vohuuhau@tdtu.edu.vn.

Dat Vinh Phat Tran received his B.Eng. degree in Automation and Control Engineering (ACE) from FEEE, TDTU in 2018. He obtained his M.Eng. degree in ACE at TDTU in 2022. He is preparing to become a Ph.D. student. His research interests include robust control of electrical drives, and building automation. He can be contacted at email: datnobita1994@gmail.com or dat.tvp@vegacity.vn.